



Effect of magnetic laponite RD on swelling and dye adsorption behaviors of κ -carrageenan-based nanocomposite hydrogels

Gholam Reza Mahdavinia^{a,*}, Zeinab Rahmani^a, Amirabbas Mosallanezhad^b, Shiva Karami^a, Mohammad Shahriari^c

^aFaculty of Science, Department of Chemistry, University of Maragheh, P.O. Box 55181-83111, Maragheh, Iran, Tel./Fax: +98 4212276060; emails: grmnia@maragheh.ac.ir (G.R. Mahdavinia), z.rahmani24@yahoo.com (Z. Rahmani), shiva.karami82@yahoo.com (S. Karami)

^bFaculty of Engineering, Department of Materials Engineering, University of Maragheh, P.O. Box 55181-83111, Maragheh, Iran, email: amirabbas.mosallanezhad@gmail.com

^cFaculty of Science, Department of Mathematics, University of Maragheh, P.O. Box 55181-83111, Maragheh, Iran, email: mohamad.shahriari@yahoo.com

Received 8 February 2015; Accepted 10 October 2015

ABSTRACT

We synthesized novel magnetic nanocomposite hydrogels of κ -carrageenan by incorporating magnetic laponite RD. The magnetite nanoparticles were embedded in laponite RD through *in situ* method. The structure of nanocomposites were characterized using X-ray diffraction, scanning electron microscopy, transmission electron microscopy, and vibrating sample magnetometer techniques. The swelling of hydrogel nanocomposites was studied and decrease in water absorbency was found by introducing magnetic laponite RD. The results indicated that the water absorbency was independent on pH of swelling media. The magnetic nanocomposites were examined as adsorbents for the removal of crystal violet (CV) from aqueous solutions. The removal of CV was investigated through batch method on the subject of contact time, initial pH of dye solution, ion strength, and initial concentration of CV. The effect of pH revealed that the adsorption process was independent of pH. Compared to the neat κ -carrageenan hydrogel (78 mg/g), the nanocomposites showed high adsorption capacity for CV due to the introduced magnetic laponite RD (164 mg/g). The adsorption isotherm data were modeled by Langmuir, Freundlich, and Dubinin–Radushkevich isotherm models. The correlation of adsorption isotherm data by mentioned models was affected by the content of magnetic laponite RD. Based on Dubinin–Radushkevich isotherm models, the adsorption process was associated with physical adsorption mechanism. Investigation of thermodynamic parameters revealed that the adsorption of CV on nanocomposites was occurred spontaneously.

Keywords: κ -Carrageenan; Magnetic; Laponite RD; Nanocomposite; Adsorption

1. Introduction

Today, adsorption technology is extensively used in many industrial fields, such as wastewater

treatment, food processing, protein purification, analytical, determinations and many other applications [1–4]. The adsorbents derived from polyionic polysaccharides have been gaining considerable attractions recently. In fact, polysaccharides are naturally

*Corresponding author.

occurring biopolymers that are extracted from renewable sources on a large scale with low cost. Due to the easy availability, many efforts have been done to prepare adsorbents derived from polysaccharides [5]. Some important polysaccharides, such as chitosan [6], sodium alginate [7], and κ -carrageenan [8], have been used in wastewater treatment especially in the removal of toxic dyes and metal ions.

Hydrogels are three-dimensional hydrophilic polymers that can absorb a large amount of aqueous solutions without dissolving in media [9]. The presence of ionic groups in the hydrogels opens potential area of application particularly removal of pollutants from wastewaters. The hydrogels composed of sodium alginate with carboxylate groups ($-\text{CO}_2^-$) [7], chitosan with pendants amine ($-\text{NH}_2$) [10], carboxymethyl cellulose with anionic carboxylate [11], κ -carrageenan with anionic sulfate groups ($-\text{OSO}_3^-$) [12] have been synthesized and evaluated as adsorbents to remove cationic dyes from wastewaters. Unfortunately, the low apparent strength of polysaccharide-based hydrogels restricts them in utilizing as appropriate adsorbent. Introduction of nanoclays, such as montmorillonite, laponite RD, and sepiolite for preparing nanocomposite adsorbents, is an easy and efficient route to overcome mentioned disadvantage [13]. In addition to clays, silica, and titanium oxide nanoparticles have been used to prepare nanocomposite hydrogels with high adsorption capacity or degradation ability for toxic dyes [2,4]. Besides, the use of magnetic adsorbents for the removal of dyes from wastewaters is attractive due to the facile separation of adsorbents from solutions using a permanent magnet [14]. The common magnetic nanoparticles used for the preparation of magnetic adsorbents are magnetite type of iron oxides (Fe_3O_4) which is synthesized from co-precipitation of $\text{Fe}^{2+}/\text{Fe}^{3+}$ iron ions. The magnetic alginate [15], chitosan [16], and κ -carrageenan [17] adsorbents have been utilized for the removal of dyes from wastewaters. Nanocomposites adsorbents comprising only nanoclays [7] or only magnetic Fe_3O_4 [17] have been applied to adsorb dye from wastes. There are just few reports in simultaneous incorporation of nanoclay and magnetite [18]. It has been reported that the laponite RD contains a large surface area with anionic centers and can make strong interactions with active ingredients [19]. Thus, in this study, we attempt to synthesize magnetic Fe_3O_4 nanoparticles through *in situ* coprecipitation of iron ions in the presence of laponite RD nanoclay. Then, the κ -carrageenan-based magnetic hydrogel nanocomposites were prepared by the incorporation of magnetic laponite RD. The structure of magnetic nanocomposite hydrogels was characterized by scanning electron microscopy (SEM), transmission

electron microscopy (TEM), X-ray diffraction (XRD), and vibrating sample magnetometer (VSM) techniques. The magnetic nanocomposite hydrogels were examined for the removal of cationic dye crystal violet from colored water. The isotherm and thermodynamic of adsorption process as well as the effect of salinity and pH on adsorption process were investigated.

2. Materials and methods

2.1. Materials

κ -Carrageenan was obtained from Condinson Co. (Denmark). Laponite RD was provided by Rockwood Additive Limited (Surface area $370 \text{ m}^2/\text{g}$, bulk density $1,000 \text{ kg}/\text{m}^3$, chemical composition: SiO_2 59.5%, MgO 27.5%, Li_2O 0.8%, Na_2O 2.8%, loss on ignition 8.2%). Acrylamide (AAm) was purchased from Nalco Chemical Co. (the Netherlands) and used after recrystallization from acetone. *N,N*-Methylenebisacrylamide (MBA, Fluka) and ammonium persulfate (APS, Merck) were used as received. The other chemicals were analytical grades and used as received.

2.2. Synthesis of Magnetic Laponite RD

About 3 g of laponite RD was dispersed in 200 mL distilled water and stirred for overnight. Then, the dispersed clay was sonicated for 10 min. The operating frequency used in sonication was 50 kHz. The iron salts (1.9 g $\text{FeSO}_4 \cdot 7\text{H}_2\text{O}$ and 3 g $\text{FeCl}_3 \cdot 6\text{H}_2\text{O}$; the $\text{Fe}^{3+}:\text{Fe}^{2+}$ ratio was 1.6) were dissolved in 20 mL of distilled water. The solution of iron salts was added to the solution of laponite RD and allowed to stir under N_2 gas for 1 h. Then, the ammonia solution (3 M) was slowly dropped into solution and allowed to reach the pH of solution to 10. The temperature of solution was adjusted at 70°C and stirred for 2 h. The solution of magnetic laponite RD was cooled to ambient temperature. The produced magnetic laponite RD was separated by permanent magnet. The product was washed with distilled water for several times until neutralization. Finally, the magnetic laponite RD was separated by magnet and the volume of solution was adjusted at 80 mL. The solution was sonicated for 10 min and a fluidly solution was obtained. The fluidly solution was used to synthesize nanocomposite hydrogels.

2.3. Synthesis of nanocomposite hydrogels

The nanocomposites based on κ -carrageenan were synthesized through grafting of acrylamide monomer onto κ -carrageenan in the presence of magnetic laponite RD and MBA crosslinker. The initial contents of

materials used to synthesize hydrogels were illustrated in Table 1. In general, different volume of fluidly magnetic laponite RD clay was dispersed in 30 mL of distilled water and allowed to stir for 24 h (speed of stirrer was 250 rpm). Then, the dispersed magnetic laponite solution was sonicated for 20 min. The operating frequency used in sonication was 75 kHz. One gram of κ -carrageenan was poured in magnetic solution and was stirred at 60°C temperature for 2 h to allow complete dissolving. Then, 3 g of AAm monomer and 0.03 g of MBA (dissolved in 2 mL of distilled water) were added into solution and allowed to complete dissolution. The obtained solution was sonicated for 5 min with the operating frequency of 25 kHz. Finally, APS initiator (0.1 g in 2 mL water) was added to the solution. After 2 h, the synthesized nanocomposite hydrogels were cut into small pieces and immersed in excess distilled water to extract unreacted components. The purified nanocomposites were dried at ambient temperature for constant weight. The dried samples were milled and sieved to 40–60 mesh sizes and kept away from light and moisture. The samples were coded as Carra (nonmagnetic hydrogel); mCarraLap1, mCarraLap2, and mCarraLap3 used 5, 10, and 20 mL fluid magnetic laponite RD for the synthesis of nanocomposite hydrogels, respectively. The nanocomposite hydrogel that synthesized by using 20 mL of fluid magnetic laponite RD without using κ -carrageenan was coded as mLap.

2.4. Swelling measurements

Dried nanocomposites were used to determine the degree of swelling. The degrees of swelling (DS) was determined by immersing the nanocomposite hydrogels (0.1 g) in distilled water (100 mL) or 0.15 M of salt solutions (50 mL) and were allowed to soak at room temperature for 24 h. After this time, they were removed from water, blotted with filter paper to remove surface water, weighed and the DS (g water/g dried nanocomposite) was calculated using Eq. (1):

$$DS = \frac{W_s - W_d}{W_d} \times 100 \quad (1)$$

where W_s and W_d are the weights of the samples swollen in water and in dry state, respectively. The effect of pH on the swelling was carried out according to above method. The pH of solutions was adjusted via dilution method by adding 0.1 M HCl or NaOH solutions.

2.5. Dye adsorption measurements

Adsorption of CV dye onto nanocomposites was carried out by immersing the 0.05 g of nanocomposites into 50 mL of dye solution with 60 mg/L of CV. All adsorption experiments were examined through a batch method on a shaker with a constant speed at 120 rpm. All the adsorption experiments were done at ambient temperature (24°C). To study the adsorption kinetics, at specified time intervals, the amount of adsorbed CV was evaluated using a UV spectrometer at $\lambda_{\max} = 590$ nm. The solutions were centrifuged (at 3,000 rpm for 10 min) before measurements. The content of adsorbed dye was calculated using Eq. (2):

$$q_t = \frac{(C_0 - C_t)}{m} \times V \quad (2)$$

where C_0 is the initial CV concentration (mg/L), C_t is the remaining dye concentration in the solution at time t , V is the volume of dye solution used (L), and m (g) is the weight of nanocomposite. Adsorption isotherm was carried out by immersing of 0.05 g of nanocomposites into 50 mL of dye solutions with 20, 40, 60, 80, 100, 150, and 200 mg/L of CV at ambient temperature (24°C) for 24 h. The equilibrium adsorption capacity of nanocomposites, q_e (mg/g), was determined using Eq. (2). At this equation, the C_t and the q_t will be replaced with equilibrium concentration of dye in the solution (C_e) and equilibrium adsorption capacity (q_e), respectively.

Table 1
Required contents of materials to synthesize of magnetic nanocomposite hydrogels

	Magnetic laponite RD (mL)	κ -Carrageenan (g)	AAm (g)	MBA (g)	APS (g)
Carra	0	1	3	0.03	0.1
mCarraLap1	5	1	3	0.03	0.1
mCarraLap2	10	1	3	0.03	0.1
mCarraLap3	20	1	3	0.03	0.1
mLap	20	0	3	0.03	0.1

The removal efficiency (RE %) of CV by nanocomposites was calculated as follows:

$$\text{RE \%} = \frac{C_0 - C_e}{C_0} \times 100 \quad (3)$$

where C_e is the remaining CV concentration in the solution at equilibrium time.

2.6. Desorption studies

Desorption study was carried out via bath method. The samples were contacted with dye solution similar to kinetic studies. The desorption solutions in this study were ethanol, water/ethanol (50/50, V/V), 0.5 M KCl in water, 0.5 M KCl in water/ethanol (50/50 m V/V), and 0.2 M acetic acid solutions. The dye-loaded mCarraLap3 nanocomposite was transferred into distilled water for 1 h in order to remove un-desorbed dye. Then, the sample was immersed into desorption solution and stirred on a shaker (120 rpm) for 24 h. Desorption content was calculated according to the calibration curve for each solution.

2.7. Instrumental analysis

Dried nanocomposites were coated with a thin layer of gold and imaged in a SEM instrument (Vega, Tescan). One-dimensional, wide-angle XRD patterns were obtained by using a Siemens D-500 X-ray diffractometer with wavelength, $\lambda = 1.54 \text{ \AA}$ (Cu $K\alpha$), at a tube voltage of 35 kV, and tube current of 30 mA. TEM micrographs were recorded with a Philips CM10 operating at 60 kV tension. The magnetic properties of the beads were studied with a VSM (model 7400, Lake-share Company, USA).

2.8. Adsorption isotherms

The data of experimental adsorption isotherms were fitted by common isotherm models. The expression of the applied non-linear Langmuir model is given by the Eq. (4) [20]:

$$q_e = \frac{q_m K_L C_e}{1 + K_L C_e} \quad (4)$$

where C_e is the equilibrium dye concentration in the solution (mg/L) at equilibrium, K_L is the Langmuir adsorption constant related to the energy of adsorption (L/mg), and q_m is the maximum adsorption capacity (mg/g).

The favorability of the adsorption process (R_L) was evaluated from the parameters of Langmuir adsorption isotherm model. The R_L can calculate from the following equation [21]:

$$R_L = \frac{1}{1 + K_L C_0} \quad (5)$$

where K_L is the Langmuir constant (L/mg) and C_0 is the initial concentration of dye. The R_L can vary: for $R_L > 1$ the adsorption is unfavorable; $R_L = 1$ the adsorption is linear condition; the adsorption is favorable when $0 < R_L < 1$; and $R_L = 0$ is for irreversible conditions [21].

In the Freundlich model, the adsorption of adsorbate occurs on a heterogeneous surface by multilayer sorption and the adsorption capacity can increase with increasing in adsorbate concentration. Nonlinear Freundlich isotherm is represented by the following equation [22]:

$$q_e = K_F C_e^{1/n} \quad (6)$$

where K_F is the equilibrium adsorption coefficient (mg/g) (L/mg) $^{1/n}$, and $1/n$ is the empirical constant. In fact, the n value depicts the favorability of adsorption process and K_F shows the adsorption capacity and intensity of the adsorbate.

The type of adsorption can be estimated from Dubinin–Radushkevich isotherm model, which is described according to the following Eq. (8) [22]:

$$q_e = q_m \exp(-\beta \times \varepsilon^2) \quad (7)$$

where q_e (mol/g) is the content of CV adsorbed on hydrogel, q_m (mol/g) is the monolayer adsorption capacity, activity coefficient β (mol 2 /kJ 2) is related to the mean adsorption energy, and ε is the Polanyi potential and its value can be calculated from Eq. (9):

$$\varepsilon = RT \ln \left(1 + \frac{1}{C_e} \right) \quad (8)$$

where C_e (mol/L) is the concentration of dye in solution at equilibrium time. The mechanism of adsorption process can be estimated from mean adsorption energy (E , kJ/mol) that is obtained from Eq. (10):

$$E = \frac{1}{\sqrt{-2\beta}} \quad (9)$$

The adsorption process occurs chemically when the E values stands between 8 and 16 kJ/mol, whereas the

adsorption process takes place physically when the E value is lower than 8 kJ/mol [23].

The nonlinear fitting of data was performed using Matlab 2013 software. The validity of models was estimated by regression coefficient (r^2 , Eq. (11)). A well fitting occurs when the r^2 is close to unity.

$$r^2 = \frac{(q_{i,\text{meas}} - \bar{q}_{i,\text{cal}})^2}{\sum_{i=1}^n (q_{i,\text{meas}} - \bar{q}_{i,\text{cal}})^2 + (q_{i,\text{meas}} - q_{i,\text{cal}})^2} \quad (10)$$

where $q_{i,\text{meas}}$ and $q_{i,\text{cal}}$ are the experimental and calculated amount of CV adsorption.

2.9. Thermodynamic parameters

The effect of temperature on the adsorption of dye onto nanocomposite was carried out at three temperatures 25, 35, and 45°C. According to the change in dye adsorption capacity by varying the temperature, the thermodynamic parameters including Gibbs free energy (ΔG , J/mol), enthalpy (ΔH , J/mol), and entropy (ΔS , J/mol) were calculated using following equations [7]:

$$K_D = \frac{C_d}{C_s} \quad (11)$$

$$\Delta G = -RT \ln K_D \quad (12)$$

$$\ln K_D = \frac{\Delta S}{R} - \frac{\Delta H}{RT} \quad (13)$$

where K_D is the equilibrium constant; C_d is the amount of adsorbed dye onto nanocomposite (mg/L) and C_s is the remained dye concentration at equilibrium time (mg/L); R is the universal gas constant (8.314 J/mol/K); and T is the absolute temperature (K).

3. Results and discussion

3.1. Synthesis and characterization

Magnetic nanocomposite hydrogels based on κ -carrageenan were synthesized through grafting of acrylamide onto κ -carrageenan by the incorporation of magnetic laponite RD. Although it has been reported that the neat laponite RD can act as crosslinker to synthesize of hydrogels [12], but after magnetization, the apparent physical strength of the obtained nanocomposite hydrogels was still low to study swelling and adsorption behaviors. So, we tried to use MBA as crosslinker to prepare magnetic nanocomposite hydrogels.

Firstly, the Fe_3O_4 magnetic nanoparticles were synthesized via *in situ* coprecipitation of $\text{Fe}^{2+}/\text{Fe}^{3+}$ ions in the presence of laponite RD nanoclay. Then, the magnetic laponite RD was added to the polymerization solution and magnetic nanocomposite were obtained. The magnetic nanocomposite hydrogels were characterized by VSM, XRD, TEM, and SEM/EDS techniques.

The morphology and surface characteristic of non-magnetic hydrogel (Carra) and magnetic nanocomposite hydrogel (mCarraLap2) was studied by SEM technique and the results shown in Fig. 1. It can be seen from micrographs that the Carra hydrogel contains a smooth and tight surface (Fig. 1(a)). The morphology of the magnetic hydrogel mCarraLap3 was similar to nonmagnetic hydrogel (Fig. 1(b)), showing well dispersing of magnetic laponite RD in hydrogel matrix. The presence of magnetic laponite RD in nanocomposite hydrogel was confirmed by EDS spectrum. The EDS of mCarraLap3 was shown in Fig. 1(c). The characteristic peak of Fe due to the magnetic Fe_3O_4 nanoparticles and characteristic peaks of silicon related to the laponite RD appeared in the EDS spectrum of magnetic hydrogel, confirming the presence of magnetic laponite RD. The XRD patterns of neat laponite RD, magnetic laponite RD, and mCarraLap3 hydrogel nanocomposite were also studied and illustrated in Fig. 1(d). The XRD profile of pristine laponite RD showed a broad peak from $2\theta = 2.5^\circ$ to $2\theta = 9.1^\circ$ with a diffraction peak at about $2\theta = 6.1^\circ$ corresponding to the $R(001)$ of clay plates with d -spacing 14.2 Å. The $R(002)$ peaks of laponite RD was appeared at $2\theta = 11.1$ with d -spacing 7.9 Å. When the magnetic Fe_3O_4 nanoparticles were synthesized through *in situ* coprecipitation of iron ions in the presence of laponite RD clay, the peak at $2\theta = 6.1^\circ$ was disappeared. Also, d -spacing of $R(002)$ was increased from 7.9 to 8.2 Å. This observation indicated the exfoliation of laponite RD plates in the presence of magnetic Fe_3O_4 nanoparticles. The existence of magnetic Fe_3O_4 nanoparticles in neat magnetic laponite RD clay was confirmed by characteristic peaks at about $2\theta = 30.3^\circ, 35.5^\circ, 43.3^\circ, 53.5^\circ, 57.2^\circ$, and 62.8° , which can be attributed to the indices (2 2 0), (3 1 1), (4 0 0), (4 2 2), (5 1 1), and (4 4 0) of magnetic Fe_3O_4 nanoparticles, respectively. Similar to neat magnetic laponite RD, the XRD patterns of magnetic nanocomposite mCarraLap3 showed characteristic peaks at $2\theta = 30.3^\circ, 35.5^\circ, 43.3^\circ, 53.5^\circ, 57.2^\circ$, and 62.8° , indicating the formation of highly crystalline and pure magnetite nanoparticles with spinel structure. The TEM image of mCarraLap3 nanocomposite was studied and the result was shown in Fig. 2(a). The laponite RD showed the plates with a lateral size of ~ 25 nm with thickness about ~ 3.5 nm (according to XRD

results). The magnetite nanoparticles with the size of lower than 3 nm were found to be embedded with clay plates. The absence of free magnetic nanoparticles can be arisen from the cation exchangeability of laponite RD that helps the nanoparticles to form on the surface and between plates of laponite RD. A similar observation has been reported by Tzitzios et al., which magnetic nanoparticles have been immobilized on laponite RD discs [24].

The hysteresis loops of neat magnetic laponite RD and magnetic nanocomposite hydrogel (mCarraLap3) were investigated using VSM technique between ± 9 kOe at 298 K. The results are depicted in Fig. 2(b). According to data, the saturation magnetizations of magnetic laponite RD and mCarraLap3 hydrogel were obtained 5.2 and 3.9 emu/g, respectively. The saturation magnetization of mCarraLap3 nanocomposite was obtained lower than that

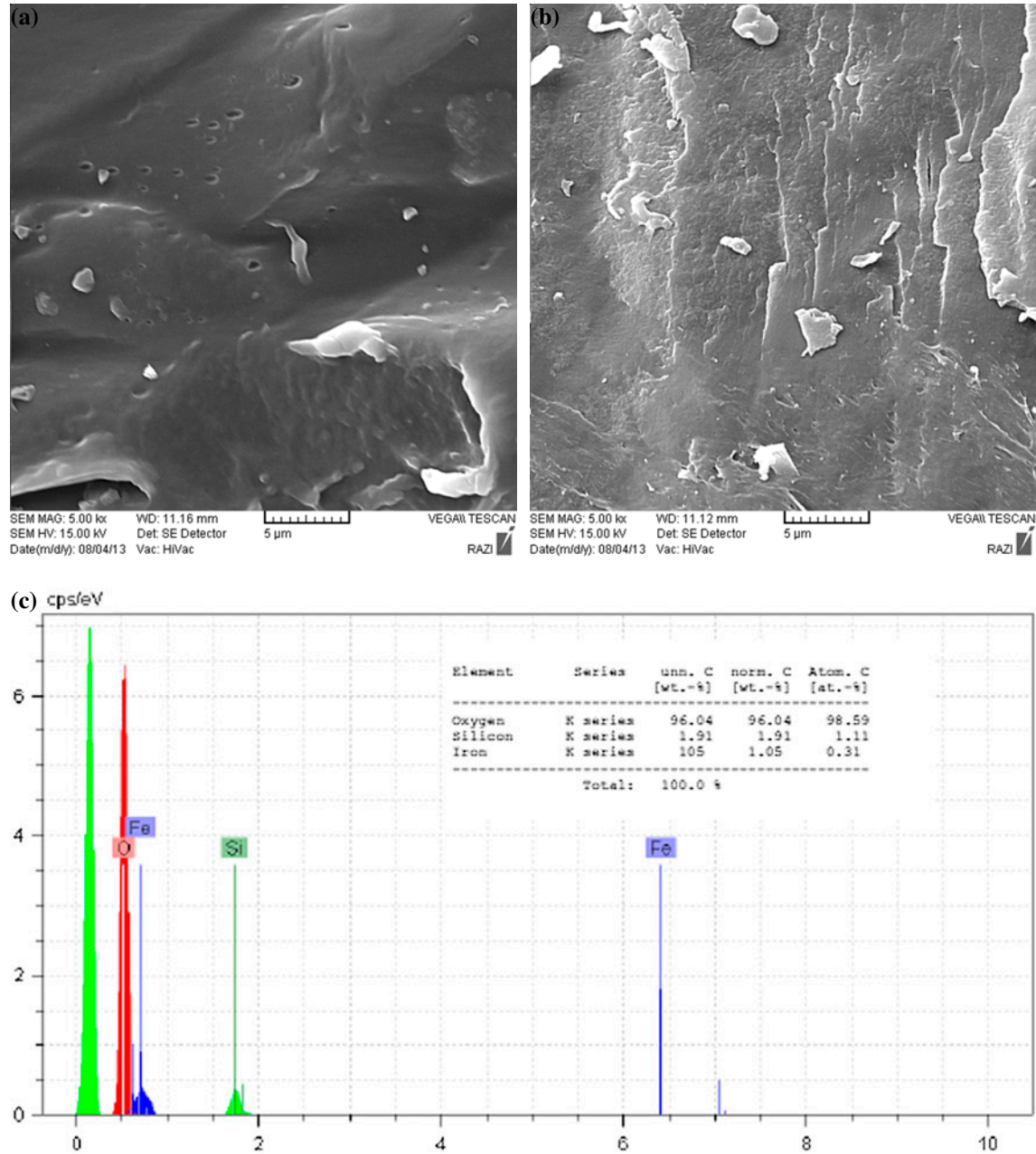


Fig. 1. SEM micrographs of Carra (a) and mCarraLap3 (b), hydrogels; EDS spectrum of mCarraLap3 (c), XRD patterns of pristine laponite RD, magnetic laponite RD, and magnetic mCarraLap3 nanocomposite hydrogel (d).

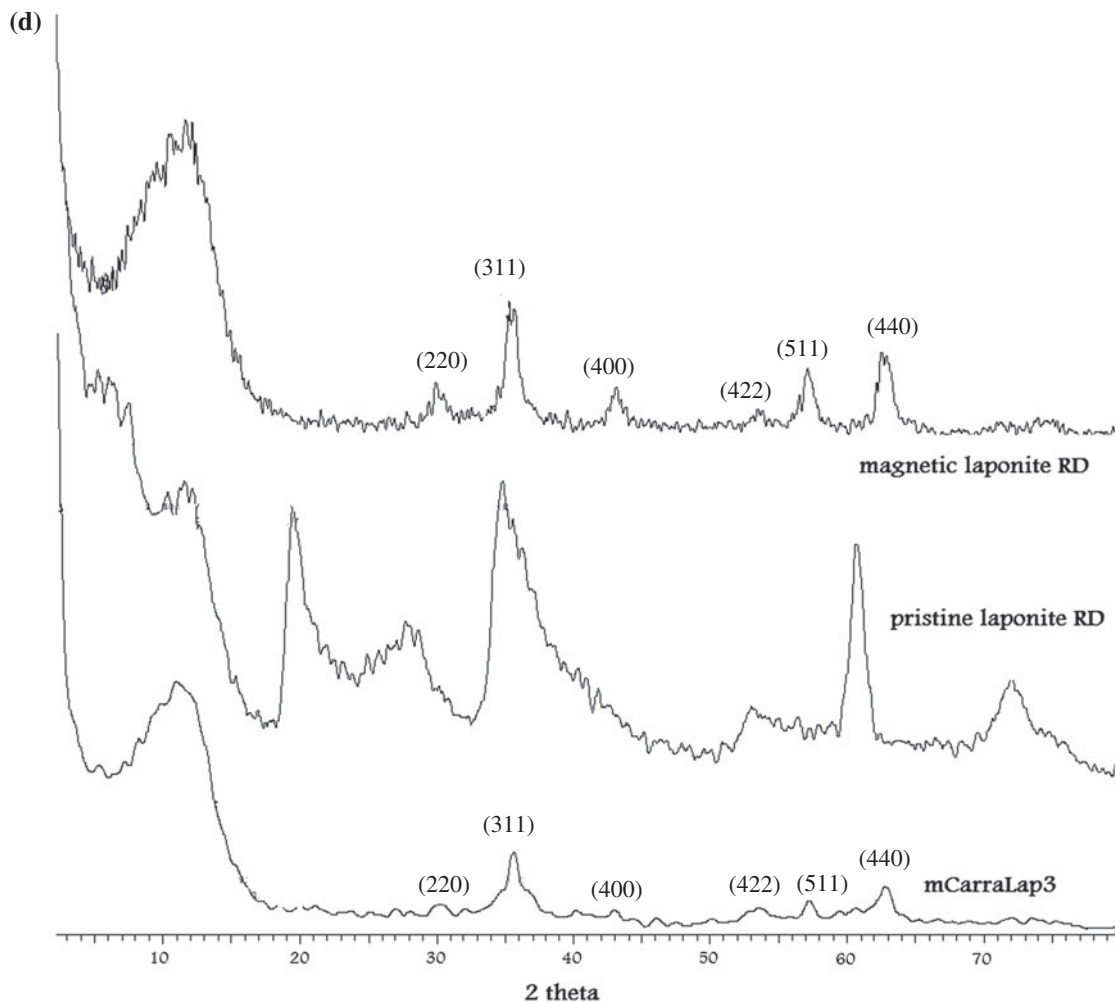


Fig. 1. (Continued).

of neat magnetic laponite RD. This observation indicates the stabilizing magnetic nanoparticles through coating by polymer matrix. After adsorption of dye onto magnetic nanocomposite, the obtained saturation magnetization of nanocomposite hydrogel was sufficient to separate the hydrogels from aqueous solution by a permanent magnet (insert of Fig. 2(b)).

3.2. Swelling study

Fig. 3(a) illustrates the swelling of nanocomposite hydrogels as a function of content of magnetic clay. The magnetic nanocomposites comprise κ -carrageenan and magnetic laponite RD. It may be noted that both osmotic pressure and repulsion between anionic sulfate groups have crucial role in the swelling of

Carra, mCarraLap1, mCarraLap2, and mCarraLap3 hydrogels. As the magnetic laponite RD was increased, the swelling of nanocomposites decreased. The corresponding decrement in swelling of nanocomposites can be attributed to this fact that the laponite RD component can act as multifunctional crosslinker [12]. With the increase in crosslinking points, the pore size of nanocomposites is decreased, and consequently, the water absorbency is reduced. The swelling capacity of mLap nanocomposite was obtained lower than those of hydrogels contained κ -carrageenan, which this observation is due to lack of anion–anion repulsions in mLap nanocomposite.

The swelling of nanocomposite hydrogels was investigated in 0.15 M of different salt solutions (Na^+ , Ca^{2+} , and Al^{3+}) with the same Cl^- counter ion (Fig. 3(a)). The nanocomposite hydrogels in this study

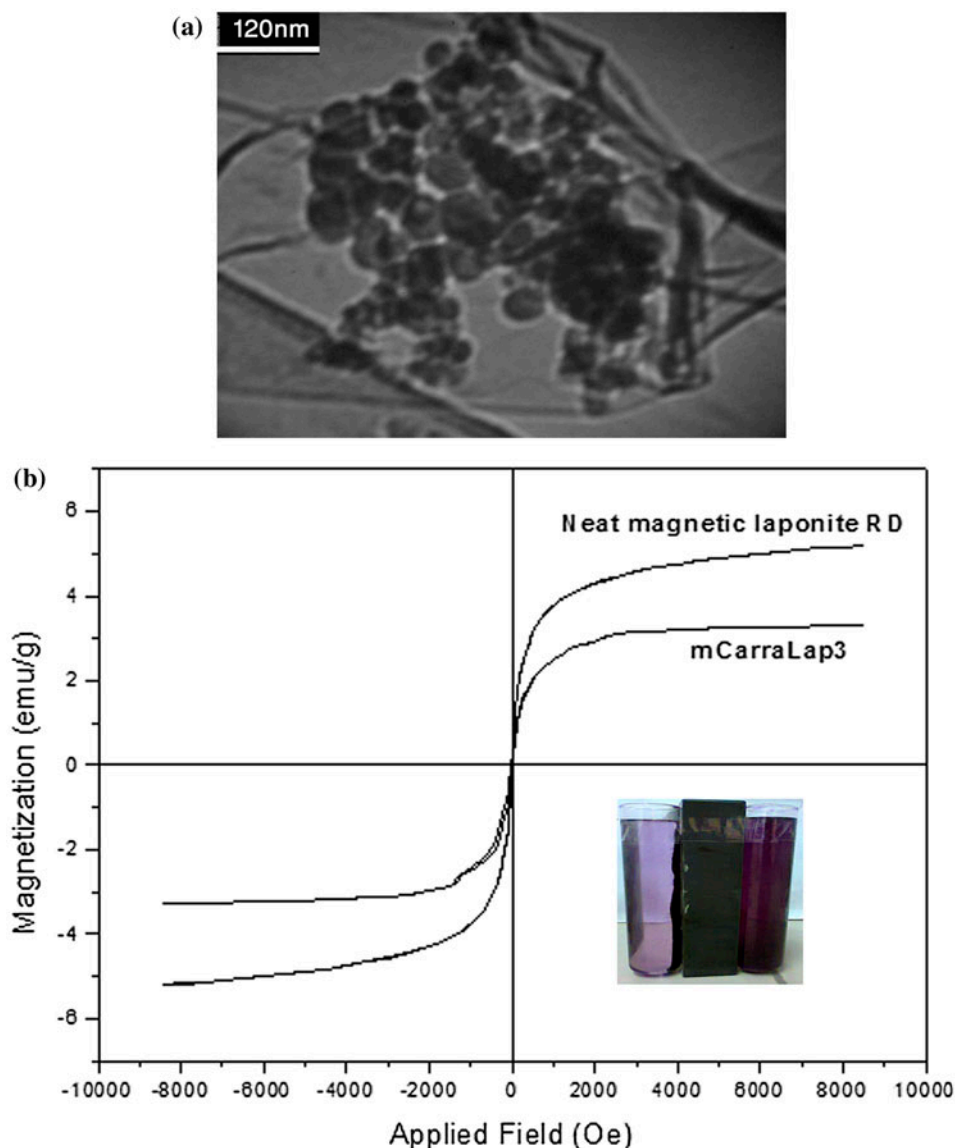


Fig. 2. TEM image of mCarraLap3 nanocomposite (a) and VSM graphs of neat magnetic laponite RD and mCarraLap3 nanocomposite hydrogel (b).

contains ionic κ -carrageenan carrying pendant sulfates, nonionic polyacrylamide component, laponite RD with anionic centers, and magnetic nanoparticles. The swelling of the ionic hydrogels in saline solutions is appreciably decreased compared to the values measured in distilled water [25]. This well-known phenomenon, commonly observed in the swelling of ionic hydrogels, is often attributed to a screening effect of the additional cations causing a nonperfect anion–anion electrostatic repulsion, leading to a decreased swelling capacity. A more reduction in water absorbency is observed at saline solutions containing multivalent cations; this observation is explained by complexing

ability arising from the coordination of the multivalent cations with anionic centers of hydrogels [26]. The swelling of hydrogels in NaCl solution indicated that the water absorbency of Carra, mCarraLap1, and mCarraLap2 hydrogels was decreased. This observation can be attributed to the screening effect of the additional Na^+ cations on anionic sulfate groups, causing a nonperfect anion–anion electrostatic repulsion. The swelling of mLap and mCarraLap3 with high content of magnetic laponite RD was not affected by the presence of NaCl. This finding may be attributed to high osmotic pressure inside corresponding hydrogels. This high osmotic pressure can be arisen from

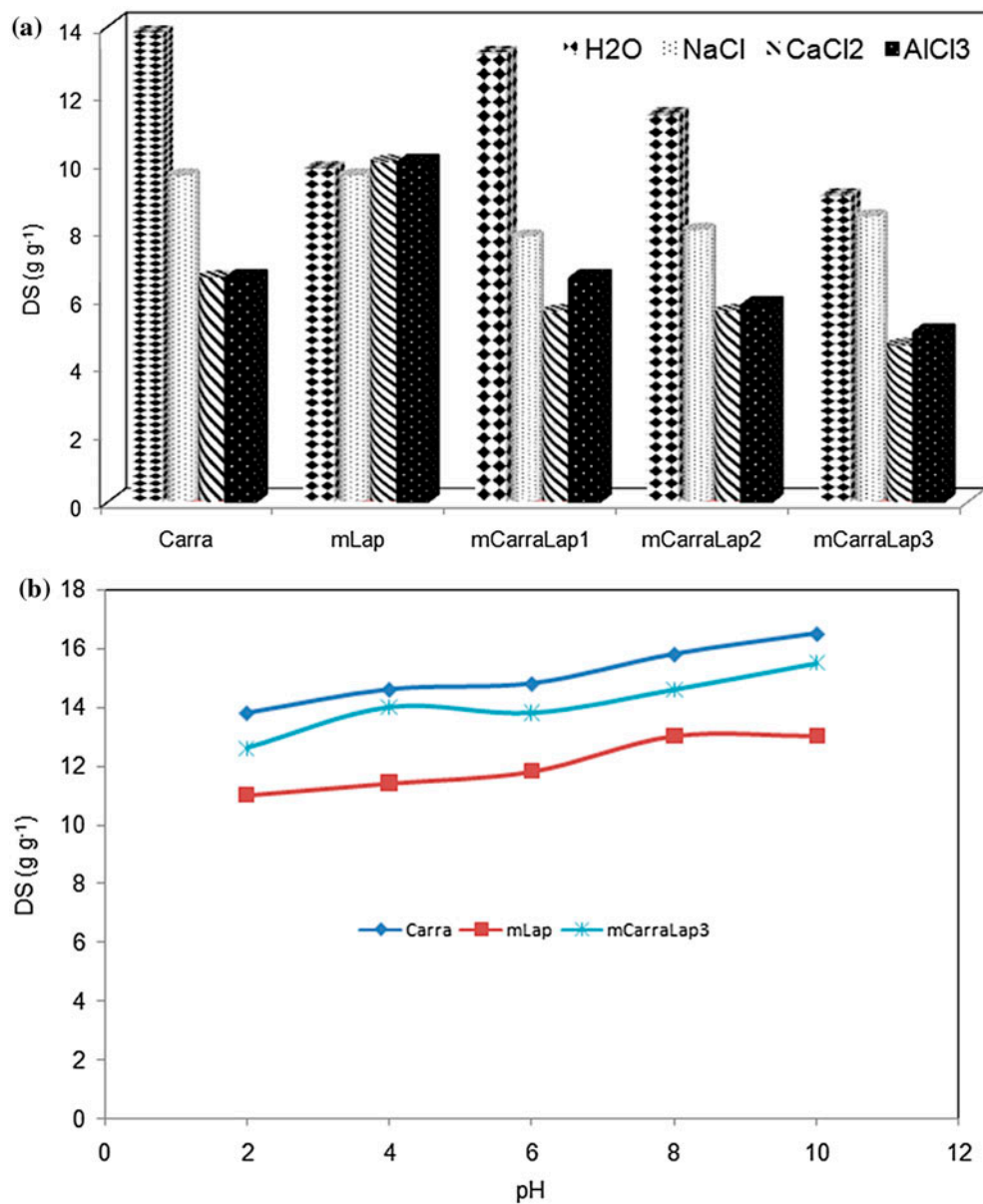


Fig. 3. Effect of magnetic laponite RD on swelling capacities of nanocomposite hydrogels in distilled water and 0.15 M of NaCl, CaCl₂, and AlCl₃ solutions (a) and effect of pH on swelling capacities of hydrogels (b).

nanometric dispersion of laponite RD plates in nanocomposite matrix. In fact, the exfoliated and intercalated laponite RD clay with anionic centers on clay can be led to an increase osmotic pressure (ionic pressure) of inside of nanocomposites. In CaCl₂ and AlCl₃ solutions, the swelling capacity of hydrogels is lower in comparison with NaCl solution. This behavior is arising from the coordination of the Ca²⁺ and Al³⁺ cations with anionic centers of hydrogels. A surprising data were achieved for mLap sample that the swelling of related hydrogel was not influenced by

type of salt solution. This observation was similar to our previous work reporting hydroxypropyl methylcellulose/laponite RD nanocomposite hydrogels [27]. To have a comparative data, a dimensionless salt sensitivity factor, f , was determined using Eq. (4) [27]:

$$f = 1 - \frac{S_s}{S_w} \quad (14)$$

where S_s and S_w are swelling in desired salt solution and in distilled water, respectively. The f -values are

also given in Table 2. Generally, in ionic nanocomposite hydrogels, hydrogel swelling in saline media is decreased. Water uptake of κ -carrageenan-based nanocomposites in saline was high and the f -values were obtained low. The low f -values indicated the lowest salt sensitivity of related nanocomposites and can be considered as antisalt nanocomposite hydrogels. The f -values of collagen-graft-poly[(acrylic acid)-*co*-(sodium acrylate)] hydrogel [28] with pendant carboxylate was compared with the nanocomposites, and according to Table 2, the f -values of the κ -carrageenan-based nanocomposites are less than collagen-based hydrogel, indicating low salt sensitivity of nanocomposites.

The effect of pH of solution on the swelling behavior of Carra, mLap, and mCarraLap3 hydrogels was investigated. The swelling data are depicted in Fig. 3(b). According to figure, none of the nanocomposites showed pH-dependent swelling behavior. κ -carrageenan is an ionic polysaccharide carrying sulfate groups ($-\text{OSO}_3^-$). These pendants are completely dissociated in the overall pH range and the hydrogels from this biopolymer shows pH-independent swelling behavior [8]. ($\text{p}K_a$ of methane sulfonic acid is ~ -2.5). So, the pH-independent behavior of nanocomposites is due to nondissociable sulfate groups. mLap indicated similar behavior. This behavior shows that the anionic centers on laponite RD cannot protonate like to weak acids. A slightly decrease in swelling of samples was observed under acidic pHs and this can be attributed to a screening effect of the additional H^+ cations causing a nonperfect anion–anion electrostatic repulsion.

3.3. Dye adsorption studies

3.3.1. Effect of contact time

The removal rates of pollutants by adsorbents are useful data to predict the required time of removal, which present the information about the efficiency of

adsorption process. Hence, the influence of contact time on the removal efficiency of CV by nanocomposites was investigated by immersing 0.05 g of adsorbents in 50 mL of CV solution with concentration of 60 mg/g. The rates of adsorption of CV on hydrogel adsorbents were shown in Fig. 4(a). Contact time plots indicated a relatively rapid removal rate. During the 195 min, the removal efficiency of dye by the mLap, mCarraLap1, mCarraLap2, and mCarraLap3, and Carra were obtained 99.1, 88, 91, 95, and 78%, respectively. The lowest content of adsorbed dye was obtained for Carra sample. The results showed that introducing magnetic laponite RD caused an improvement in the content of adsorbed CV on nanocomposites. This result can be arisen from this fact that the laponite RD comprises a large surface area ($330 \text{ m}^2/\text{g}$) with anionic centers and can makes strong interactions with active ingredients [19]. In fact, the affinity of magnetic laponite RD for CV was higher than that of carrageenan.

3.3.2. Effect salinity and pH on adsorption

The adsorption capacities of adsorbents can be affected by the ion strength of dye solutions [29]. To investigate the effect of salinity on the adsorption capacities of Carra, mLap, and mCarraLap3 hydrogels, the ion strength of dye solution (60 mg/g) was adjusted by different concentration of NaCl. Depending on the content of magnetic laponite RD, the adsorption of CV on corresponding samples showed different trends (Fig. 4(b)). The CV adsorption on mCarraLap3 and mLap remained invariant with an increase in the NaCl concentration. In contrast, a decrement was found for the CV adsorption on the Carra. The corresponding reduction of CV adsorption on the Carra may be attributed to the low swelling of adsorbents in NaCl solutions. The low swelling of Carra leads to a decreased surface area and so a reduction in adsorption of dye on hydrogels is

Table 2

Degree of swelling and salt sensitivity (f -values) of nanocomposite hydrogels in distilled water and 0.15 M of salt solutions

	$\text{DS}_{\text{H}_2\text{O}}$	DS_{NaCl}	$\text{DS}_{\text{CaCl}_2}$	$\text{DS}_{\text{AlCl}_3}$	f_{NaCl}	f_{CaCl_2}	f_{AlCl_3}
Carra	13.8	9.6	6.6	6.5	0.3	0.52	0.52
mLap	9.8	9.6	10	10	0.02	−0.02	−0.02
mCarraLap1	13.2	7.8	5.6	5.8	0.41	0.57	0.56
mCarraLap2	11.4	8	5.6	5.8	0.3	0.51	0.49
mCarraLap3	9	9.4	4.6	5	−0.04	0.48	0.44
Collagen-based nanocomposite ^a	1,200	73	8	5	0.94	0.9	1

^aCollagen-graft-poly[(acrylic acid)-*co*-(sodium acrylate)] hydrogel.

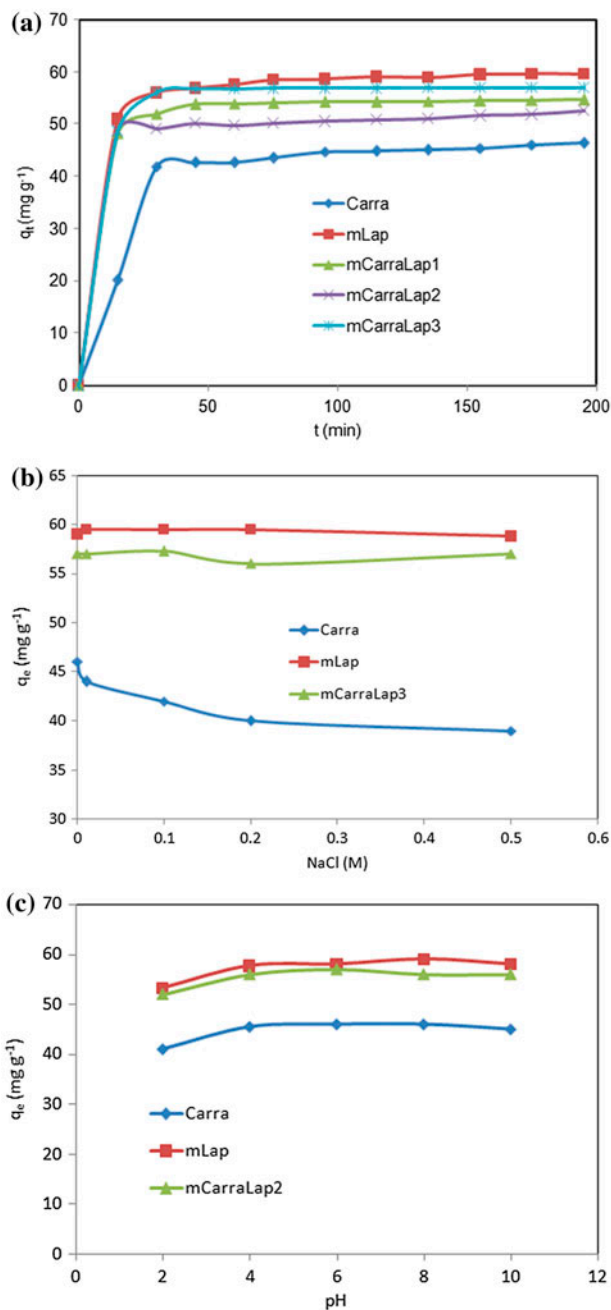


Fig. 4. Effect of contact time on adsorption of CV on hydrogels (a), effect of NaCl concentration on adsorption capacities of hydrogels (b) and influence of pH of initial dye solution on dye adsorption capacities of hydrogels (c).

observed. According to Fig. 3(a), contrary to the Carra hydrogel, the degrees of swelling of mLap and mCarraLap3 were relatively equal in both NaCl solution and distilled water, and no reduction in surface area is observed.

The effect of the pH of initial dye solution on the adsorption capacity of adsorbents was also studied. In

order to investigate the influence of pH, the pH of dye solutions changed from 2 to 10 and the results are indicated in Fig. 4(c). The variation in dye adsorption capacity of studied adsorbents was not remarkable. This observation was in agreement with our previous work, which described the magnetic κ -carrageenan/PVA adsorbents [7]. The pHs of point zero charge (pH_{pzc}) of carrageenan-based hydrogels were obtained lower than 2. So, the sulfate pendants on hydrogels are in dissociated form when the pH of solution be equal or higher than 2. On the other hands, the carrageenan-based adsorbents are negatively charged at pH range of 2–10. Similar to Carra hydrogel, the adsorption capacities of magnetic nanocomposites containing magnetic laponite RD were not changed by varying the pH of initial dye solution. According to the investigation reported by Jatav and Joshi, the pH of laponite solutions is increased due to the released OH^- ions from edge of clay [30]. Thus, the pH of dye solutions with the initial pHs of 2 and 4 were measured after equilibrium (24 h), and the final pHs were found to be higher than 5.5. So, the invariant dye adsorption capacities of hydrogels comprising carrageenan and laponite RD can be assigned to the low pH_{pzc} of carrageenan and also to the increased pH of dye solutions owing to the released OH^- ions from laponite clay.

3.4. Adsorption isotherms

The influence of initial CV concentration on the adsorption capacity of nanocomposites was investigated. The results can be used to study the adsorption isotherm that explains the correlation between the content of adsorbed dye on nanocomposites and the remained dye in solution at equilibrium time [31]. Fig. (5) indicates the relationship between equilibrium adsorption capacity of hydrogels (Carra, mCarraLap2, and mLap) and the remaining dye in solution. At lower initial CV concentration, the main fraction of dye is adsorbed on the adsorbents; whereas at higher dye concentration, the adsorption capacity of hydrogels remains constant that can be attributed to the saturation of active centers on adsorbents. The types of interactions between adsorbate molecules and adsorbent surface can be studied by adsorption isotherms. The experimental data were discussed according to nonlinear Langmuir, Freundlich, and Dubinin–Radushkevich isotherm models. In the Langmuir adsorption model, adsorption of adsorbate takes place at specific homogeneous sites within the adsorbent and valid for monolayer adsorption on adsorbents.

The experimental isotherm data of Carra, mCarraLap2, and mLap were compared with described

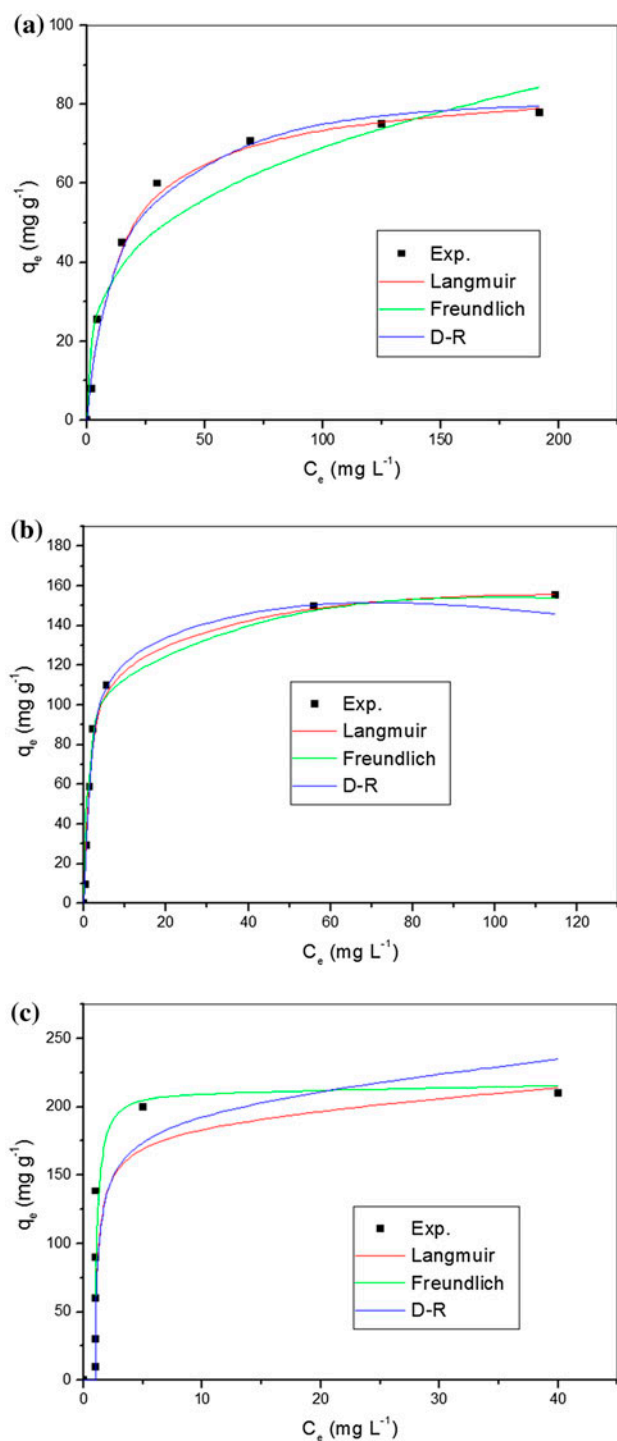


Fig. 5. Comparison of equilibrium isotherms between the experimental data and theoretical data from isotherm models for adsorption of CV on Carra (a), mCarralap2 (b), and mLap (c).

isotherm models and the results were shown in Fig. 5. While the experimental data of Carra obeyed well the Langmuir model, a contrary trend was observed for

mCarraLap2 (well fitting for both Langmuir and Freundlich models) and mLap (well fitting to the Freundlich model). The values of r^2 and the adsorption constant parameters calculated according to the isotherm models were summarized in Table 3. The r^2 values demonstrated that the agreement of isotherm models with experimental data was affected by the presence of magnetic laponite RD component. The adsorption of CV on Carra and mCMCLap1 hydrogels followed well the Langmuir model, whereas the nanocomposite comprised high content of magnetic laponite RD (mCarraLap2, mCarraLap3, and mLap) followed well both Langmuir and Freundlich isotherm models. Unlike mCarraLap2 and mCarraLap3 that follow well both Langmuir and Freundlich models, the mLap adsorbent conform the Freundlich model the best. The R_L values were between 0 and 1 and indicated that the adsorption of CV on hydrogels was favorable. Besides, the n parameter in Freundlich model was between 1 and 10, which indicated the favorability of adsorption process. It can be seen from by calculating mean adsorption energies from D-R isotherm model, the E values were found to be lower than 6 kJ/mol, indicating that the mechanism of adsorption of CV on all samples is physical in nature.

The enhanced adsorption capacity of nanocomposite hydrogels due to the introduced high content of magnetic laponite RD may be attributed to the well correlation of experimental data with Freundlich model. In our previous works, we reported nanocomposite hydrogels by the incorporation of neat laponite RD clay. The adsorption of CV onto HPMC/laponite RD [27] and κ -carrageenan/laponite RD [12] nanocomposite hydrogels showed that the experimental isotherm data followed well Langmuir model and maximum adsorption capacities were obtained 80.2 and 77 mg/g for κ -carrageenan/laponite RD and HPMC/laponite RD, respectively. In this study, the experimental adsorption capacities of mCarraLap1, mCarraLap2, mCarraLap3, and mLap for CV were found to be 110, 155, 164, and 210 mg/g, respectively. Thus, the following adsorption isotherm data from Freundlich and subsequent multilayer adsorption of CV on samples (against monolayer adsorption in Langmuir model) may be a reason for enhanced dye adsorption capacity of present samples [32].

3.5. Thermodynamic of adsorption

According to Eq. (13), the ΔH and ΔS can be calculated from slope and intercept of linear plot of $\ln K_D$ vs. $1/T$, respectively (Fig. 6, mCarraLap2). The results were summarized in Table 4. The negative ΔG values indicate that adsorption of dye onto nanocomposite

Table 3

Freundlich, Langmuir, and D–R isotherm parameters for the adsorption of CV on hydrogels

Isotherm	Parameters	Carra	mCarraLap1	mCarraLap2	mCarraLap3	mLap
Freundlich	n	3.5	4.34	4.4	3.68	9
	K_F	19.4	35.8	57.4	51.16	140
	r^2	0.92	0.85	0.97	0.98	0.98
Langmuir	q_m	82	108.1	160	172.3	208
	b	0.093	0.2534	0.447	0.2541	0.218
	r^2	0.99	0.97	0.98	0.99	0.78
D–R	q_m	69.3	102	147.3	159.7	197
	β	0.067	0.0205	0.0138	0.01915	0.081
	E	2.7	4.9	6	5.1	0.0977
	r^2	0.94	0.956	0.98	0.955	2.26

takes place spontaneously. In addition, the increment in values of ΔG revealed that by increasing temperature, the adsorption of CV on nanocomposite can be less favorable. The negative value of ΔH indicates that the adsorption process occurs exothermically. Also, the negative value of enthalpy shows decreased randomness at the solid-solution interface.

The mechanism of adsorption of dye on nanocomposites could be estimated from the values of ΔG and ΔH [33,34]. The values of ΔG ranging from -20 to 0 kJ/mol indicate that the physisorption is dominated; but chemisorption is occurred for a range of -80 to -400 kJ/mol. By considering the ΔG values in Table 4, it is concluded that in this study the mechanism of adsorption process is physisorption. In addition, the values of ΔH lower than 20 kJ/mol depicts that the physisorption interactions such as Van der Waals are dominated. The values of ΔH ranging from 20 to 80 kJ/mol indicate that the physisorption interaction

Table 4

Thermodynamic parameters for adsorption of CV on mCarraLap2 hydrogel

T (K)	ΔS (J/K/mol)	ΔH (kJ/mol)	ΔG (kJ/mol)	R^2
298	-63.4	-26.4	-7.2	0.99
308			-6.8	
318			-6.2	

such as electrostatic leads to the adsorption of adsorbate on adsorbent. The chemisorption interaction occurs when the values of ΔH are between 80 and 450 kJ/mol. The enthalpy value for the adsorption of CV on magnetic nanocomposite was obtained -26.4 kJ/mol. According to the ΔH value for the adsorption process, the positive CV dye molecules adsorb electrostatically on the anionic centers of magnetic nanocomposite [32].

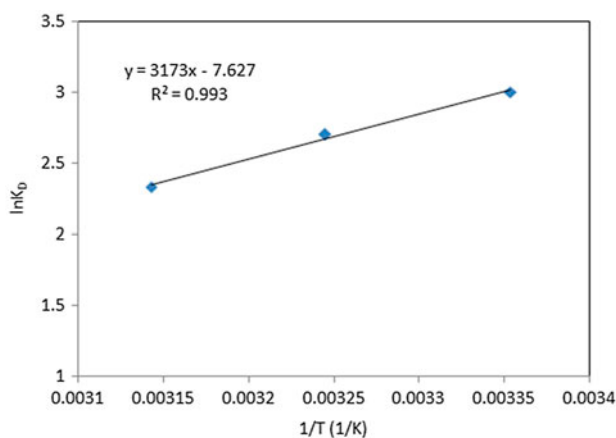


Fig. 6. The plot between $\ln K_D$ against $1/T$ to obtain the thermodynamic parameters.

3.6. Desorption–adsorption cycles

In addition to the high adsorption capacity of adsorbents for dyes, the regeneration ability of adsorbents is an important factor for reusing. So, we attempt to evaluate desorption of adsorbed dye using different solutions (Fig. 7(a)). Ethanol (96% V/V), 0.5 M of KCl solution, 50/50 V/V of ethanol/water mixture, and 0.5 M of KCl in 50/50 V/V of ethanol/water mixture were used to study for desorbing of dye from nanocomposites. Desorption efficiencies by various solutions were illustrated in Fig. 7(a). Firstly, desorption was examined with 0.5 M KCl solution and the desorbing of dye was negligible. The desorbing percentage of dye using 96% V/V of ethanol was obtained 39%. The replacing of desorption solution by ethanol/water mixture (50/50 V/V), desorption efficiency was achieved 30%.

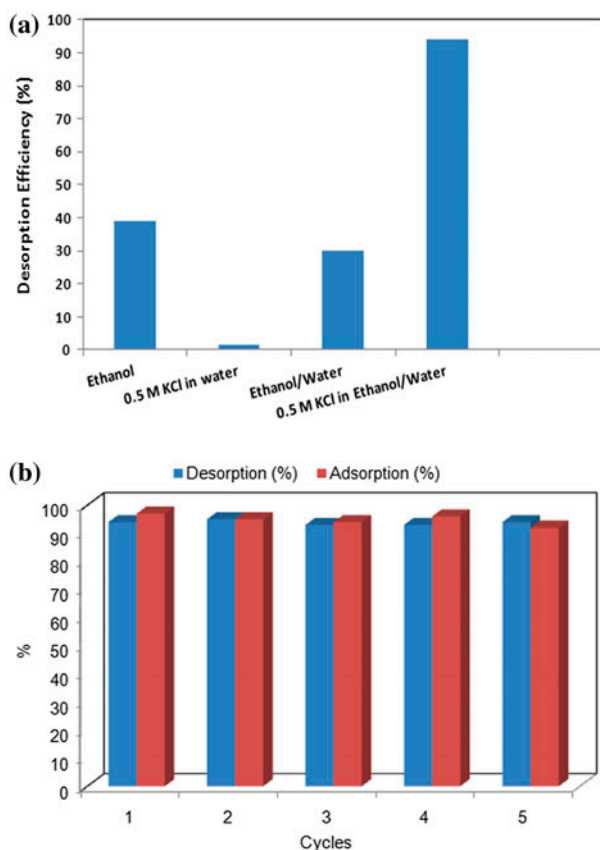


Fig. 7. Effect of solvent type on desorption of CV from mCarraLap3 (a) and desorption–adsorption efficiencies of CV from mCarraLap3 during 5 cycles (b).

Desorption efficiency of dye using above solutions was not sufficient for practical applications. So, we tried to investigate the desorbing of dye by combination of KCl and ethanol/water mixture. By immersing the nanocomposite containing dye into 0.5 M of KCl in ethanol/water, desorption efficiency was efficiently increased and obtained more than 94%. According to this observation, we endeavored to study the desorption–adsorption process for 5 times by using KCl in ethanol/water as regeneration agent. During five cycles, the nanocomposite mCarraLap3 indicated almost the same dye adsorption capacity and the changing in desorption efficiency and adsorption capacity was negligible (Fig. 7(b)). In fact, the results indicated that the nanocomposites can be used for multiple cycles without decreasing in adsorption capacity for CV dye.

4. Conclusion

The magnetic hydrogels were synthesized by the incorporation of kappa-carrageenan and magnetic

laponite RD, where magnetic laponite RD were obtained through *in situ* co-precipitation of iron ions in the presence of laponite RD clay. The structural characterization was done by XRD, SEM, TEM, and VSM techniques. The swelling experiments indicated that the water absorbency of magnetic nanocomposites was affected by the content of magnetic laponite RD. In distilled water, the swelling capacity was decreased by increasing the magnetic clay. Dye adsorption results revealed that the removal of dye was strongly increased by introducing magnetic laponite RD. Also, the influence of initial pH of dye solution indicated that the adsorption capacity of hydrogels was not changed remarkably. Freundlich, Langmuir, and D–R isotherm models were employed to analysis the batch adsorption experimental data. By the incorporation of magnetic laponite RD, the experimental adsorption isotherm data were followed well both Langmuir and Freundlich models. The values of mean adsorption energy (obtainable from D–R isotherm model) indicated physical adsorption process, which was confirmed by the ΔH value obtained from thermodynamic parameters. According to the thermodynamic parameters, the adsorption of CV dye on adsorbents occurred spontaneously. The results demonstrated that the nanocomposites can be used for multiple cycles without decreasing in adsorption capacity for CV. In comparison to the common industrial adsorbents, the polysaccharide-based adsorbents are expensive. This disadvantage can be overcome by the high adsorption capacity of polysaccharide-based pollutants. The corresponding kappa-carrageenan nanocomposite hydrogels showed high adsorption capacity for CV.

References

- [1] S. Li, Removal of crystal violet from aqueous solution by sorption into semi-interpenetrated networks hydrogels constituted of poly(acrylic acid-acrylamide-methacrylate) and amylose, *Bioresour. Technol.* 101 (2010) 2197–2202.
- [2] H. Mittal, A. Maity, S.S. Ray, Synthesis of co-polymer-grafted gum karaya and silica hybrid organic–inorganic hydrogel nanocomposite for the highly effective removal of methylene blue, *Chem. Eng. J.* 279 (2015) 166–179.
- [3] W.H. Yu, N. Li, D.S. Tong, C.H. Zhou, C.X. Lin, C.Y. Xu, Adsorption of proteins and nucleic acids on clay minerals and their interactions: A review, *Appl. Clay Sci.* 80–81 (2013) 443–452.
- [4] S. Pal, A.S. Patra, S. Ghorai, A.K. Sarkar, V. Mahato, S. Sarkar, R.P. Singh, Efficient and rapid adsorption characteristics of templating modified guar gum and silica nanocomposite toward removal of toxic reactive blue and Congo red dyes, *Bioresour. Technol.* 191 (2015) 291–299.

- [5] R.S. Blackburn, Natural polysaccharides and their interactions with dye molecules: Applications in effluent treatment, *Environ. Sci. Technol.* 38 (2004) 4905–4909.
- [6] Y.T. Zhou, H.L. Nie, C. Branford-White, Z.Y. He, L.M. Zhu, Removal of Cu^{2+} from aqueous solution by chitosan-coated magnetic nanoparticles modified with α -ketoglutaric acid, *J. Colloid Interface Sci.* 330 (2009) 29–37.
- [7] G.R. Mahdavinia, H. Aghaie, H. Sheykhoie, M.T. Vardini, H. Etemadi, Synthesis of CarAlg/MMt nanocomposite hydrogels and adsorption of cationic crystal violet, *Carbohydr. Polym.* 98 (2013) 358–365.
- [8] G.R. Mahdavinia, A. Massoudi, A. Baghban, E. Shokri, Study of adsorption of cationic dye on magnetic *kappa*-carrageenan/PVA nanocomposite hydrogels, *J. Environ. Chem. Eng.* 2 (2014) 1578–1587.
- [9] G.R. Mahdavinia, A. Pourjavadi, H. Hosseinzadeh, M.J. Zohuriaan, Modified chitosan 4. Superabsorbent hydrogels from poly(acrylic acid-co-acrylamide) grafted chitosan with salt- and pH-responsiveness properties, *Eur. Polym. J.* 40 (2004) 1399–1407.
- [10] G.J. Copello, A.M. Mebert, M. Raineri, M.P. Pesenti, L.E. Diaz, Removal of dyes from water using chitosan hydrogel/SiO₂ and chitin hydrogel/SiO₂ hybrid materials obtained by the sol-gel method, *J. Hazard. Mater.* 186 (2011) 932–939.
- [11] G. Zhang, L. Yi, H. Deng, P. Sun, Dyes adsorption using a synthetic carboxymethyl cellulose-acrylic acid adsorbent, *J. Environ. Sci.* 26 (2014) 1203–1211.
- [12] G.R. Mahdavinia, A. Massoudi, A. Baghban, B. Massoumi, Novel carrageenan-based hydrogel nanocomposites containing laponite RD and their application to remove cationic dye, *Iran. Polym. J.* 21 (2012) 609–619.
- [13] E.I. Unuabonah, A. Taubert, Clay-polymer nanocomposites (CPNs): Adsorbents of the future for water treatment, *Appl. Clay Sci.* 99 (2014) 83–92.
- [14] S. Li, X. Liu, W. Huang, W. Li, X. Xia, S. Yan, J. Yu, Magnetically assisted removal and separation of cationic dyes from aqueous solution by magnetic nanocomposite hydrogels, *Polym. Adv. Technol.* 22 (2011) 2439–2447.
- [15] N.M. Mahmoodi, Magnetic ferrite nanoparticle-alginate composite: Synthesis, characterization and binary system dye removal, *J. Taiwan Inst. Chem. Eng.* 44 (2013) 322–330.
- [16] D.H.K. Reddy, S.M. Lee, Application of magnetic chitosan composites for the removal of toxic metal and dyes from aqueous solutions, *Adv. Colloid Interface Sci.* 201–202 (2013) 68–93.
- [17] G.R. Mahdavinia, S. Irvani, S. Zoroufi, H. Hosseinzadeh, Magnetic and K^+ -cross-linked *kappa*-carrageenan nanocomposite beads and adsorption of crystal violet, *Iran. Polym. J.* 23 (2014) 335–344.
- [18] L. Jiang, P. Liu, Design of magnetic attapulgite/fly ash/poly(acrylic acid) ternary nanocomposite hydrogels and performance evaluation as selective adsorbent for Pb^{2+} ion, *ACS Sustainable Chem. Eng.* 2 (2014) 1785–1794.
- [19] Y. Li, D. Maciel, H. Tomás, J. Rodrigues, H. Ma, X. Shi, pH sensitive Laponite/alginate hybrid hydrogels: swelling behaviour and release mechanism, *Soft Matter* 7 (2011) 6231–6238.
- [20] K.Y. Foo, B.H. Hameed, Insights into the modeling of adsorption isotherm systems, *Chem. Eng. J.* 156 (2010) 2–10.
- [21] K. Hall, L.C. Eagleton, A. Acrivos, T. Vermeulen, Pore- and solid-diffusion kinetics in fixed-bed adsorption under constant-pattern conditions, *Ind. Eng. Chem. Fundam.* 5 (1966) 212–223.
- [22] E.S. Dragan, D.F.A. Loghin, A.I. Cocarta, Efficient sorption of Cu^{2+} by composite chelating sorbents based on potato starch-graft-polyamidoxime embedded in chitosan beads, *ACS Appl. Mater. Interfaces* 6 (2014) 16577–16592.
- [23] S. Vasiliu, I. Bunia, S. Racovita, V. Neagu, Adsorption of cefotaxime sodium salt on polymer coated ion exchange resin microparticles: Kinetics, equilibrium and thermodynamic studies, *Carbohydr. Polym.* 85 (2011) 376–387.
- [24] V. Tzitzios, G. Basina, A. Bakandritsos, C.G. Hadjipanayis, H. Mao, D. Niarchos, G.C. Hadjipanayis, J. Tucek, R. Zboril, Immobilization of magnetic iron oxide nanoparticles on laponite discs—An easy way to biocompatible ferrofluids and ferrogels, *J. Mater. Chem.* 20 (2010) 5418–5428.
- [25] H. Omidian, S.A. Hashemi, P.G. Sammes, I. Meldrum, Modified acrylic-based superabsorbent polymers (dependence on particle size and salinity), *Polymer* 40 (1999) 1753–1761.
- [26] G.R. Mahdavinia, A. Pourjavadi, H. Hosseinzadeh, M.J. Zohuriaan, Modified chitosan 4. Superabsorbent hydrogels from poly(acrylic acid-co-acrylamide) grafted chitosan with salt- and pH-responsiveness properties, *Eur. Polym. J.* 40 (2004) 1399–1407.
- [27] G.R. Mahdavinia, F. Bazmizyynabad, Synthesis of anti-salt hydroxypropyl methylcellulose-g-polyacrylamide/Laponite RD nanocomposite hydrogel and its application to remove cationic dye, *Polym.-Plast. Technol. Eng.* 53 (2014) 411–422.
- [28] G.B. Marandi, S. Hariri, G.R. Mahdavinia, Effect of hydrophobic monomer on the synthesis and swelling behaviour of a collagen-graft-poly[(acrylic acid)-co-(sodium acrylate)] hydrogel, *Polym. Int.* 58 (2009) 227–235.
- [29] P.L. Tan, C.L. Wong, S.L. Hii, Investigation on adsorptive removal of basic dye by seaweed-derived biosorbent: Considering effects of sorbent dosage, ionic strength and agitation speed, *Desalin. Water Treat.* 48 (2012) 238–244.
- [30] S. Jatav, Y.M. Joshi, Chemical stability of Laponite in aqueous media, *Appl. Clay Sci.* 97–98 (2014) 72–77.
- [31] F. Marahel, M.A. Khan, E. Marahel, I. Bayesti, S. Hosseini, Kinetics, thermodynamics, and isotherm studies for the adsorption of BR2 dye onto avocado integument, *Desalin. Water Treat.* 53 (2015) 826–835.
- [32] Y. Zheng, A. Wang, Preparation and ammonium adsorption properties of biotite-based hydrogel composites, *Ind. Eng. Chem. Res.* 49 (2010) 6034–6041.
- [33] A. Ozcan, E.M. Oncu, A. Ozcan, Adsorption of Acid Blue 193 from aqueous solutions onto DEDMA-sepiolite, *J. Hazard. Mater.* 129 (2006) 244–252.
- [34] F.M. Machado, C.P. Bergmann, T.H.M. Fernandes, E.C. Lima, B. Royer, T. Calvete, S.B. Fagan, Adsorption of Reactive Red M-2BE dye from water solutions by multi-walled carbon nanotubes and activated carbon, *J. Hazard. Mater.* 192 (2011) 1122–1131.